n−σ Charge-Transfer Interaction and Molecular and Electronic Structural Properties in the Hydrogen-Bonding Systems Consisting of *p*-Quinone Dianions and Methyl Alcohol

Bunji Uno,*[,†] Noriko Okumura,[†] Masashi Goto,[†] and Kenji Kano[‡]

Gifu Pharmaceutical University, Mitahora-higashi, Gifu 502-8585, Japan, and Division of Applied Life Sciences, Graduate School of Agriculture, Kyoto University, Sakyo-ku, Kyoto 606-8502, Japan

Received October 13, 1999

Molecular and electronic structural properties of the hydrogen-bonded complexes of *p*-quinone dianions (PQ^{2-}) were investigated by electrochemistry and spectroelectrochemistry of PQ in MeCN combined with ab initio MO calculations. Hydrogen bonding between PQ^{2-} and MeOH was measured as the continuous positive shift of the apparent second half-wave reduction potentials with increasing concentrations of MeOH. Detailed analyses of the behavior reveal that PQ^{2-} forms the 1:2 hydrogen-bonded complexes at low concentrations of MeOH and the 1:4 complexes at high concentrations, yielding the formation constants. Temperature dependence of the formation constants allows us to yield the formation energy as 76.6 and 118.9 kJ mol^{-1} for the 1:2 and 1:4 complex formation of the 1,4-benzoquinone dianion (BQ^{2-}) with MeOH, respectively. These results show that the π-dianions involving the quinone carbonyl groups exhibit very strong hydrogen-accepting ability. The longest wavelength band of the spectra of BQ^{2-} and the chloranil dianion (CL^{2-}) is assigned to the $^1B_{3u} \leftarrow {}^1A_g$ band mainly contributed from an intramolecular charge-transfer (CT) configuration. Hydrogen bonding allows the band of BQ^{2-} and CL^{2-} to be blue-shifted, depending on the strength of the hydrogen bonds. CNDO/S-CI calculations reveal that the blue shift is ascribed to stabilization of the ground state by the hydrogen bonding involving strong n−σ-type CT interaction. The HF/6-31G(d) calculation results show that the structure of PQ^{2-} is characterized by a lengthening of the C═O bonds and a benzenoid ring. The geometrical properties of the hydrogen-bonded complexes of PQ^{2-} are a slight lengthening of the C═O bonds and a short distance of the hydrogen bonds. It is demonstrated that this situation is due to the strong n−σ CT interaction in the hydrogen bonds. The results suggest that the differing functions and properties of biological quinones are conferred by the n−σ CT interaction through hydrogen bonding of the dianions with their protein environment.

Introduction

Hydrogen bonding of quinones has been found to play an important role in controlling both intra- and intermolecular structures in biological systems and biological functions as an active site of quinoenzymes.[1−4] In this regard, the hydrogen bonds are being used in redox-mediated molecular recognition systems by virtue of the differences in their strength and directionality in the redox states of quinones.[5] The electrochemical and spectroelectrochemical investigations on the redox quinone systems involving the equilibria of electron transfer coupled with the hydrogen bonding give much information concerning the effect of molecular structure and environment on these basic processes. The quinone dianion has, however, been investigated in terms of quinone−hydroquinone couples as prototypical examples of organic redox systems.[6−8] In addition to the interest in their intrinsic chemical and biochemical aspects, studies on the hydrogen bonds of quinone dianions are particularly important in terms of gaining understanding of a coupler of electron and proton transfers in energy-transducing membranes for respiration and photosynthesis.[2−4] In the reaction-center of protein complexes of photosynthetic bacteria and plant Photosystem II there are two kinds of quinones termed Q_a and Q_b.[2] It is well recognized that Q_a and Q_b act in concert to enable efficient charge separation to take place, and their differing functions and properties are conferred by their interactions with the protein environment. Differences in the hydrogen-bonding ability of both quinones and the reduced products involving Q_b^{2-} working as a two-electron carrier are generally put forward for the differing functions observed. A variety of spectroscopies have been applied to characterize quinones in quinoenzymes and the reaction center in photosynthesis.[9,10] To understand the structure−function relationships from the spectra observed in such studies, it is essential to characterize reduced quinones in view of hydrogen bonding. In recent years, hydrogen bonding of the 1,4-benzoquinone (BQ)

* To whom correspondence should be addressed. E-mail: uno@gifu-pu.ac.jp.
† Gifu Pharmaceutical University.
‡ Kyoto University.

(1) Swallow, A. J. In *Function of Quinones in Energy Conserving Systems*; Trumpower, B. L., Ed; Academic Press: New York, 1982; Chapter 3.
(2) Okamura, M. Y.; Feher, G. *Annu. Rev. Biochem.* **1992**, *61*, 881.
(3) Klinman, J. P.; David, M. *Annu. Rev. Biochem.* **1994**, *63*, 299.
(4) Ding, H.; Moser, C. C.; Robertson, D. E.; Tokito, M. K.; Daldal, F.; Dutton, P. L. *Biochemistry* **1995**, *34*, 11606.
(5) Niemz, A.; Rotello, V. M. *Acc. Chem. Res.* **1999**, *32*, 44.
(6) Chambers, J. Q. In *The Chemistry of the Quinoid Compounds*; Patai, S., Rappoport, Z., Eds.; Wiley: New York, 1988; Vol. II; 1974; Vol I.
(7) (a) Peover, M. E. In *Electroanalytical Chemistry*; Bard, A. J., Ed.; Dekker: New York, 1967; pp 1−51. (b) Peover, M. E. *J. Chem. Soc.* **1962**, 4540. (c) Kolthoff, I. M.; Lingane, J. *J. Polarography*, 2nd ed.; Interscience: New York, 1952; Vol. I and II.
(8) Gupta, N.; Linschitz, H. *J. Am. Chem. Soc.* **1997**, *119*, 6384.

10.1021/jo991590q CCC: $19.00
Published on Web 02/16/2000

radical anion and dianion has been actively investigated for such reasons.[11−15]

In this study, the structural and spectral properties of the *p*-quinones dianions (PQ^{2-}) and their hydrogen-bonded complexes with MeOH were examined by electrochemical and spectroelectrochemical measurements and ab initio MO calculations. The electronic spectra and the structure of the quinone dianions and their hydrogen-bonded complexes have not been fully analyzed yet. To provide basic data for analysis of the structure of the hydrogen-bonded complexes and strength of the hydrogen bond of biological quinone dianions, we used simple systems consisting of PQ^{2-} and MeOH as a prototype of the hydrogen-bonding systems.

Experimental Section

Chemicals. The PQ employed here were BQ, 1,4-naphthoquinone (NQ), 9,10-anthraquinone (AQ), chloranil (CL), and bromanil (BR), which were commercially available from Nacalai Tesque, Inc. BQ, NQ, and AQ were purified by repeated sublimation under reduced pressure and once again just before use.[16] Recrystallization from Me_2O was adopted for the purification of CL and BR. MeOH of spectrograde purity from Nacalai Tesque was stored over molecular sieves (3A, Nacalai) for more than 2 days and then carefully rectified prior to use. The solvent used for spectral and electrochemical measurements was MeCN of spectrograde purity, which was purified as reported in a previous paper.[17] Tetrapropylammonium perchlorate (TPAP) was prepared as described previously[17] and used as a supporting electrolyte for MeCN. TPAP was dried well under high vacuum just before use.

Electrochemical and Spectral Measurements. Cyclic voltammetry was performed with a three-electrode system consisting of a Metrohm EA-290 hanging mercury drop working electrode or a glassy carbon (GC) working electrode, a coiled platinum counter electrode, and a saturated calomel reference electrode (SCE). The voltammograms were recorded with a BAS 100B electrochemical workstation, coupled to a FMV-5133D7 PC and BAS electrochemical software to record and analyze the data. Temperature was controlled during the measurements by circulating constant-temperature ethanol throughout the cell compartment by the use of a Tokyo Rikakikai thermoleader, model UA-100. The sample solutions were prepared in a drybox completely filled with N_2 gas to prevent contamination by moisture. The solutions were purged with N_2 gas to remove oxygen, and N_2 gas was passed over the solution during the measurements. Other details of the electrochemical measurements and the experimental procedures were described in previous papers.[16,17]

Spectral measurements for the neutral species were done in the usual manner with a Hitachi 323 spectrophotometer equipped with a cell holder temperature-controlled by circulating constant-temperature ethanol supplied from a Taiyo EZL-80 thermoleader. Electronic spectra of the electrogenerated dianions were observed by a method involving rapid circulation of the electrolyzed solution via a Shimadzu SPD-M10A photodiode array detector with the optical path length of 1.0 cm, coupled to a Gateway P5-100 PC and Shimadzu M10A software to record and analyze the data.[13] Controlled-potential electrolyses were performed in a bulk electrolysis cell with a Hokuto Denko HA-501 potentiostat in a three-electrode mode consisting of a reticulated vitreous carbon working electrode, an $Ag/AgNO_3$ reference electrode (containing CH_3CN solution of 0.1 M tetrabutylammonium perchlorate and 0.01 M $AgNO_3$; BAS), and a coiled platinum wire counter electrode. The details of the spectroelectrochemical measurements were described in a previous paper.[13]

MO Calculations. The geometries for PQ, PQ^-, and PQ^{2-} and their hydrogen-bonded complexes with MeOH were gradient optimized at the SCF level with the Gaussian98 program.[18,19] For the closed-shell neutral and dianionic species, the geometries were fully optimized in the RHF framework with 6-31G(d) basis sets. The optimized geometries for the neutral species were in good agreement with the results obtained from X-ray crystallographic analyses.[20] The geometries for the open-shell doublet anions were obtained in the UHF framework by gradient techniques with 6-31G(d) basis sets. Optimization of the 1:4 hydrogen-bonded complexes of NQ^{2-} and AQ^{2-} with MeOH was, however, not possible because of computer cost. The energies of the hydrogen bonds were calculated at the SCF and MP2 levels. The post-SCF calculations were done with the geometries optimized at the SCF level. The 6-31+G(d,p) basis sets at the SCF and MP2 levels were used to get the results for BQ and the reduced products with higher accuracy.

Semiempirical CNDO/S-CI calculations were carried out to interpret the spectral characteristics and the electronic states of BQ, BQ^{2-}, CL, and CL^{2-} and their hydrogen-bonded complexes with MeOH. The parameters necessary for the calculations were taken from the literature of Jaffé's group and others.[21] Two-center repulsion integrals were evaluated using the Nishimoto−Mataga equation.[22] Only the one-electron transition was taken into account for CI calculations. The optimized molecular geometries obtained by the RHF/6-31G(d) calculations were used for the calculations.

Results and Discussion

Dependence of Cyclic Voltammograms of PQ upon Concentrations of MeOH. It is well-known that quinones show typically two cathodic polarographic waves, which correspond to sequential formation of the anion radicals and dianions. The energetics of these steps have been discussed on the basis of MO theory in previous papers.[17,23] In these reductions, the first and

(9) (a) van den Brink, J. S.; Spoyalov, A. P.; Gast, P.; van Liemt, W. B. S.; Raap, J.; Lugtenburg, J.; Hoff, A. J. *FEBS Lett.* **1994**, *353*, 272. (b) Breton, J.; Brie, J.-R.; Boullais, C.; Nabedryck, E.; Mioskowski, C. *Biochemistry* **1994**, *33*, 14378. (c) Breton, J.; Boullais, C.; Berger, G.; Mioskowski, C.; Nabedryk, E. *Biochemistry* **1995**, *34*, 11606. (d) van Liemt, W. B. S.; Boender, G. J.; Gast, P.; Hoff, A. J.; Lugtenberg, J.; de Groot, H. M. *J. Biochemistry* **1995**, *34*, 10229.

(10) Zhao, X.; Ogura, T.; Okamura, M.; Kitagawa, T. *J. Am. Chem. Soc.* **1997**, *119*, 5263.

(11) Zhao, X.; Imahori, H.; Zhan, C. G.; Sakata, Y.; Iwata, S.; Kitagawa, T. *J. Phys. Chem. A* **1997**, *101*, 622.

(12) Uno, B.; Kawabata, A.; Kano, K. *Chem. Lett.* **1992**, 1017.

(13) Okumura, N.; Uno, B. *Bull. Chem. Soc. Jpn.* **1999**, *72*, 1213.

(14) O'Malley, P. J. *J. Phys. Chem. A* **1997**, *101*, 9813.

(15) O'Malley, P. J. *J. Phys. Chem. A* **1997**, *101*, 6334.

(16) Uno, B.; Kano, K.; Konse, T.; Kubota, T.; Matsuzaki, S.; Kuboyama, A. *Chem. Pharm. Bull.* **1985**, *33*, 5155.

(17) Kubota, T.; Kano, K.; Uno, B.; Konse, T. *Bull. Chem. Soc. Jpn.* **1987**, *60*, 3865.

(18) Frisch, M. J.; Trucks, G. W.; Schlegel, H. B.; Scuseria, G. E.; Robb, M. A.; Cheeseman, J. R.; Zakrzewski, V. G.; Montgomery, J. A.; Stratmann, R. E., Jr.; Burant, J. C.; Dapprich, S.; Millam, J. M.; Daniels, A. D.; Kudin, K. N.; Strain, M. C.; Farkas, O.; Tomasi, J.; Barone, V.; Cossi, M.; Cammi, R.; Mennucci, B.; Pomelli, C.; Adamo, C.; Clifford, S.; Ochterski, J.; Petersson, G. A.; Ayala, P. Y.; Cui, Q.; Morokuma, K.; Malick, D. K.; Rabuck, A. D.; Raghavachari, K.; Foresman, J. B.; Cioslowski, J.; Ortiz, J. V.; Baboul, A. G.; Stefanov, B. B.; Liu, G.; Liashenko, A.; Piskorz, P.; Komaromi, I.; Gomperts, R.; Martin, R. L.; Fox, D. J.; Keith, T.; Al-Laham, M. A.; Peng, C. Y.; Nanayakkara, A.; Gonzalez, C.; Challacombe, M.; Gill, P. M. W.; Johnson, B.; Chen, W.; Wong, M. W.; Andres, J. L.; Gonzalez, C.; Head-Gordon, M.; Replogle, E. S.; Pople, J. A. *Gaussian 98*, Pittsburgh, 1998.

(19) Foresman, J. B.; Frisch, Æ. *Exploring Chemistry with Electronic Structure Methods*, 2nd ed.; Gaussian, Inc.: Pittsburgh, 1993.

(20) (a) Trotter, J. *Acta Crystallogr.* **1960**, *13*, 86. (b) Ganltier, P. J.; Hauw, C. *Acta Crystallogr.* **1965**, *18*, 179. (c) Murty, B. V. R. *Z. Kristallogr.* **1960**, *113*, 445.

(21) (a) Ellis, R. L.; Kuehnlenz, G.; Jaffé, H. H. *Theor. Chim. Acta* **1972**, *26*, 131. (b) Kuehnlenz, G.; Jaffé, H. H. *J. Chem. Phys.* **1973**, *58*, 2238. (c) Tinland, B. *Mol. Phys.* **1969**, *16*, 413. (d) Lipari, N. O.; Duke, C. B. *J. Chem. Phys.* **1975**, *63*, 1768. (e) Jacques, P.; Faure, J.; Chalvet, D.; Jaffé, H. H. *J. Phys. Chem.* **1981**, *85*, 473.

(22) Mataga, N.; Nishimoto, K. *Z. Physik. Chem.* **1957**, *13*, 140.

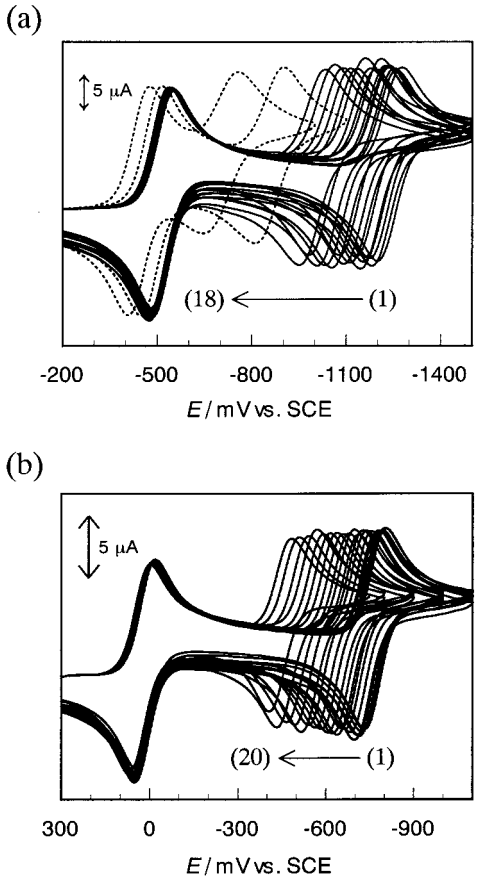

Figure 1. Cyclic voltammograms of 5.04×10^{-4} M BQ (a) and 4.37×10^{-4} M CL (b) in the absence and the presence of MeOH in MeCN containing 0.1 M TPAP, recorded with a GC electrode at a scan rate of 100 and 50 mV s^{-1} for (a) and (b), respectively. The voltammograms 17 and 18 in (a) are denoted by a dotted line. (a) [MeOH] (M): (1) 0.00, (2) 1.23×10^{-3}, (3) 2.47×10^{-3}, (4) 3.70×10^{-3}, (5) 4.93×10^{-3}, (6) 6.16×10^{-3}, (7) 8.63×10^{-3}, (8) 1.11×10^{-2}, (9) 1.48×10^{-2}, (10) 1.85×10^{-2}, (11) 2.47×10^{-2}, (12) 3.21×10^{-2}, (13) 4.19×10^{-2}, (14) 5.55×10^{-2}, (15) 7.40×10^{-2}, (16) 9.86×10^{-2}, (17) 2.34×10^{-1}, (18) 6.78×10^{-1}. (b) [MeOH] (M): (1) 0.00, (2) 1.24×10^{-3}, (3) 3.70×10^{-3}, (4) 6.47×10^{-3}, (5) 1.11×10^{-2}, (6) 1.85×10^{-2}, (7) 3.21×10^{-2}, (8) 5.42×10^{-2}, (9) 7.27×10^{-2}, (10) 9.74×10^{-2}, (11) 1.28×10^{-1}, (12) 1.71×10^{-1}, (13) 2.33×10^{-1}, (14) 3.07×10^{-1}, (15) 4.06×10^{-1}, (16) 5.29×10^{-1}, (17) 6.77×10^{-1}, (18) 8.99×10^{-1}, (19) 1.23, (20) 1.60.

second steps are reversible or at least quasireversible at customary scan rates even in the presence of MeOH as a weak proton donor. Typical voltammograms are shown in Figure 1. It is clearly found that both of the waves of BQ are significantly shifted to the positive direction with increasing concentrations of MeOH ([MeOH]), as shown in Figure 1a. Certainly, the effect of the hydrogen bonds on first redox potentials has been well recognized, particularly in the case of redox proteins as flavoproteins.[24−26] We have ascribed the significant potential shift of the second wave to specific BQ^{2-}−MeOH interaction (i.e., hydrogen bonding) in a previous paper.[12] This

Scheme 1. Equilibria Involving Two-Step One-Electron Transfer and Formation of the Hydrogen-Bonded Complexes with MeOH

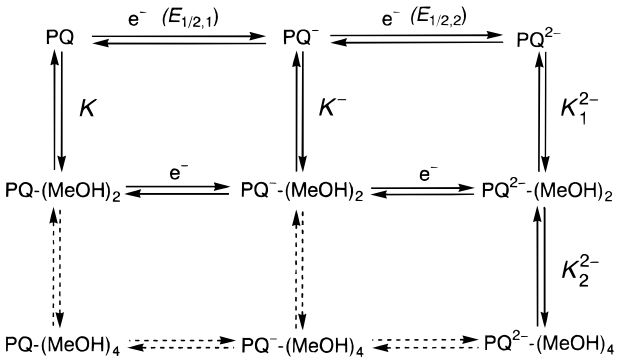

propensity is apparently observed for the second wave corresponding to the BQ^{2-} generation even at [MeOH] less than 10^{-2} M. No effect of addition of MeOH on the first wave of BQ is observed at [MeOH] less than 10^{-2} M. These findings imply that BQ^{2-} easily forms the hydrogen-bonded complex with MeOH compared to BQ and BQ^{-}. When [MeOH] exceeds 1 M, the second wave begins to merge with the first wave. The same voltammetric behaviors were observed for NQ and AQ. On the other hand, a qualitatively similar but small effect of addition of MeOH on the waves of CL was observed, as shown in Figure 1b. The second wave is not merged to the first wave in a high [MeOH] region and even in MeOH itself. The quite small shift of the first wave of CL is observed even at a higher [MeOH] region than 1 M. This fact indicates that the hydrogen-accepting ability of CL^{-} and CL^{2-} is weaker than that of BQ^{-} and BQ^{2-}, respectively. The quantitatively same behavior was observed in the cyclic voltammograms of BR.

Formation Constants and Formation Energies of the Hydrogen-Bonded Complexes of PQ, PQ^{-}, and PQ^{2-} with MeOH. The two-point hydrogen-bonding model is reasonable for the PQ and PQ^{-} complexes with MeOH.[27] This model is generally accepted for a variety of hydrogen-bonding systems involving PQ.[27−29] Recently, O'Malley has supported the symmetrical 1:4 hydrogen-bonded complex model of BQ^{-} with MeOH on the basis of the effect of hydrogen bonding on the spin density distribution and hyperfine couplings of BQ^{-} in MeOH.[14] This suggests that the hydrogen-bonding model of PQ^{2-} involves the 1:4 complex formation in view of the strength and directionality of the hydrogen bonds of PQ^{2-}. Scheme 1 shows the sequential two-step one-electron redox equilibria involving the 1:2 complex formation of PQ^{2-} with MeOH as well as PQ and PQ^{-} and the 1:4 complex formation of PQ^{2-}.

The systematic changes in the UV spectra were recorded in MeCN with addition of various concentrations of MeOH to PQ solutions, showing clear isosbestic points resulting from quite specific interaction without changes

(23) Uno, B.; Matsuhisa, Y.; Kano, K.; Kubota, T. *Chem. Pharm. Bull.* **1984**, *32*, 1.
(24) (a) Galus, G. *Fundamentals of Electrochemical Analysis*; Ellis Harwood: Chichester, 1976; Chapter 14. (b) Chauhan, B. G.; Fawcett, W. R.; Lasia, A. A. *J. Phys. Chem.* **1977**, *81*, 1476. (c) Fawcett, W. R.; Opallo, M.; Fedurco, M.; Lee, J. W. *J. Am. Chem. Soc.* **1993**, *115*, 196. (d) Peover, M. E. *J. Chem. Soc.* **1962**, 4540.
(25) Ge, Y.; Lilienthal, R. R.; Smith, D. K. *J. Am. Chem. Soc.* **1996**, *118*, 3976.
(26) (a) Caffrey, M. S.; Daldal, F.; Holden, H. M.; Cusanovich, M. A. *Biochemistry* **1991**, *30*, 4119. (b) Goodin, D. B.; McRee, D. E. *Biochemistry* **1993**, *32*, 3313. (c) Huang, J.; Ostrander, R. L.; Rheingold, A. L.; Walters, M. A. *Inorg. Chem.* **1995**, *34*, 1090.
(27) Joesten, M. D. *Hydrogen Bonding*; Marcel Dekker: New York, 1974.
(28) Aoyama, Y.; Asakura, M.; Matsui, Y.; Ogoshi, H. *J. Am. Chem. Soc.* **1991**, *113*, 6233.
(29) Nishimoto, K. In *Biomolecules Electronic Aspects*; Nagata, C., Hatano, M., Tanaka, J., Suzuki, H., Eds.; Japan Sci. Soc. Press: Tokyo, Elsevier: Amsterdam, 1985; pp 9−19.

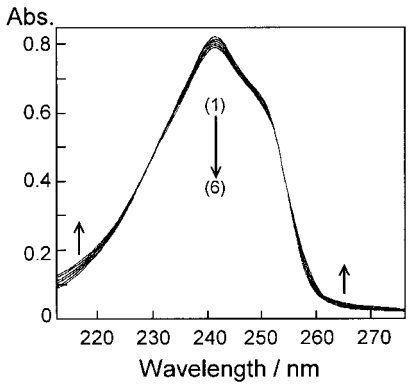

Figure 2. Electronic spectra of 3.67×10^{-5} M BQ at various concentrations of MeOH in MeCN. [MeOH] (M): (1) 0.00, (2) 4.93×10^{-1}, (3) 9.75×10^{-1}, (4) 1.46, (5) 1.95, (6) 2.46.

in bulk polarity, as shown in Figure 2. Under the conditions of the 1:2 hydrogen-bonded complex formation equilibria and of an excess of [MeOH] compared with the total concentration of PQ, the following equation is adopted to yield the formation constants (K)[30]

$$\epsilon = \frac{1}{K}\frac{\epsilon_{PQ} - \epsilon}{[MeOH]^2} + \epsilon_C \quad (1)$$

where the values of ϵ_{PQ}, ϵ_C, and ϵ represent the absorption coefficients of the free and complexed PQ (PQ−$(MeOH)_2$) and the apparent one, respectively. The ϵ vs $(\epsilon_{PQ} - \epsilon)/[MeOH]^2$ plots were approximately on straight lines with a correlation coefficient of more than 0.97, and the K values were easily obtained from the slope of the lines, the results being summarized in Table 1.

To quantify the binding of PQ^- and PQ^{2-} with MeOH, we noted the dependence of the first and second half-wave reduction potentials upon [MeOH]. Postulating that the diffusion coefficients are equal through PQ, PQ^-, and PQ^{2-} and their hydrogen-bonded complexes, the [MeOH] dependence of the $\Delta E_{1/2,n}$ values ($n = 1$ and 2 for the first and second waves, respectively) is written as follows by adaptation of the Nernstain relation for the equilibria shown in Scheme 1[31,32]

$$\Delta E_{1/2,1} = -\frac{RT}{F}\ln\frac{1 + K[MeOH]^2}{1 + K^-[MeOH]^2} \quad (2)$$

$$\Delta E_{1/2,2} = -\frac{RT}{F}\ln\frac{1 + K^-[MeOH]^2}{1 + K_1^{2-}[MeOH]^2 + K_1^{2-}K_2^{2-}[MeOH]^4} \quad (3)$$

where the $\Delta E_{1/2,n}$ values are defined as $\Delta E_{1/2,n} = E'_{1/2,n} - E_{1/2,n}$, $E_{1/2,n}$ and $E'_{1/2,n}$ being the half-wave reduction potentials of PQ themselves and the apparent half-wave potentials in the presence of MeOH, respectively, taken as the midpoint between the cathodic and anodic peak potentials of the cyclic voltammograms. The sum of eqs 2 and 3 leads to

$$\Delta E_{1/2,1} + \Delta E_{1/2,2} = -\frac{RT}{F}\ln\frac{1 + K[MeOH]^2}{1 + K_1^{2-}[MeOH]^2 + K_1^{2-}K_2^{2-}[MeOH]^4} \quad (4)$$

By analogy with this treatment, we write the following equations when only the 1:2 complex formation (eq 5) and only the 1:4 complex formation (eq 6) are considered.

$$\Delta E_{1/2,1} + \Delta E_{1/2,2} = -\frac{RT}{F}\ln\frac{1 + K[MeOH]^2}{1 + K_1^{2-}[MeOH]^2} \quad (5)$$

$$\Delta E_{1/2,1} + \Delta E_{1/2,2} = -\frac{RT}{F}\ln\frac{1 + K[MeOH]^2}{1 + K^{2-}[MeOH]^4} \quad (6)$$

Here, K^{2-} is defined as $K^{2-} = K_1^{2-}K_2^{2-} = [PQ^{2-}-(MeOH)_4]/[PQ^{2-}][MeOH]^4$. We analyzed the experimental data on the basis of eqs 4−6 to yield the formation constants of PQ^{2-} using the K values listed in Table 1. Figures 3 and 4 show typical examples of the nonlinear plots for BQ and CL, respectively. It is clearly indicated that neither eq 5 nor 6 explains the potential shift on addition of various concentrations of MeOH, as shown in Figures 3a and 4a. Equations 5 and 6 clearly explain the apparent half-wave reduction potentials in low and high [MeOH] regions, respectively, as is seen from Figures 3b and 4b. The results show that the smooth onset of the positive shift of the waves is ascribed to the 1:2 hydrogen-bonded complex formation in the low [MeOH] region and the linear increase of $(\Delta E_{1/2,1} + \Delta E_{1/2,2})$ values to log[MeOH] values results from the 1:4 complex formation in the high [MeOH] region. Indeed, the excellent curve-fitting results are obtained on the basis of eq 4, as shown in Figures 3b and 4b (represented by a solid line). The values of K_1^{2-} and K_2^{2-} are collected in Table 1. The $K_1^{2-} \cdot K_2^{2-}$ values are in good agreement with the K^{2-} values obtained from the regression analyses based on eq 6 for the data in the high [MeOH] regions (more than 1.85×10^{-2} and 3.07×10^{-1} for BQ and CL, respectively). These imply that the hydrogen bonding initially occurs at two points of the carbonyl oxygen atoms, which is distinguishable from the 1:4 hydrogen-bonded complex formation. The quite large values of K_1^{2-} and K_2^{2-} indicate that PQ^{2-} strongly attracts weak hydrogen-donors such as alcohols, compared to PQ, PQ^- and other organic molecules. Although errors in measurements of the small changes in $E'_{1/2,1}$ led to uncertainties in the estimation of K^- values, the K^- values for BQ^-, NQ^-, and AQ^- were obtained from the analyses based on eq 3, as listed in Table 1.

Temperature dependence of the formation constants allows us to yield $\Delta H°$ and $\Delta S°$ values for the hydrogen-bonded complex formation of PQ and their reduced species from the slope of the linear relation between $-R \ln K'$ and $1/T$ values, where K' denotes the formation constants (K, K^-, K_1^{2-}, and K_2^{2-}). The results show that the hydrogen bonds of the dianions are considered as strong enthalpy-driven stabilization, as listed in Table 1. In addition, the results indicate that reduction of PQ to PQ^- to PQ^{2-} controls the strength of the hydrogen bonds.

Electronic Absorption Spectra of PQ^{2-} and the Hydrogen-Bonded Complexes with MeOH. Spectro-

(30) Kubota, T. *J. Am. Chem. Soc.* **1965**, *87*, 458.
(31) Meites, L. *Polarographic Techniques*, 2nd ed.; John Wiley: New York, 1965; Chapter 5, pp 267−284.
(32) (a) Kano, K.; Mori, K.; Uno, B.; Goto, M.; Kubota, T. *J. Am. Chem. Soc.* **1990**, *112*, 8645. (b) Kano, K.; Mori, K.; Uno, B.; Kutota, T. *J. Electroanal. Chem.* **1990**, *283*, 187.

Table 1. Thermodynamic Data of the Hydrogen-Bonded Complexes of PQ and Their Reduced Species with MeOH in MeCN

		formation constants/dm^6 mol^{-2}					
compd		288.0 K	293.0 K	298.0 K	303.0 K	$\Delta H°$/kJ mol^{-1}	$\Delta S°$/J mol^{-1} K^{-1}
BQ	K	1.02	8.70×10^{-1}	7.50×10^{-1}	6.40×10^{-1}	−19.9	−69.0
BQ^-	K^-		3.3×10^a	$2.5 \times 10^{a,c}$	1.9×10^a	-42^a	-110^a
BQ^{2-}	K_1^{2-}		4.98×10^4	$3.10 \times 10^{4\ c}$	1.77×10^4	−76.6	−171
	K_2^{2-}		5.88×10^2	4.61×10^2	3.32×10^2	−42.3	−90.8
NQ	K	2.27	2.07	1.72^c		−19.7	−61.5
NQ^-	K^-	4.9×10^a	4.2×10^a	$2.9 \times 10^{a,c}$		-39^a	-100^a
NQ^{2-}	K_1^{2-}	1.05×10^5	7.22×10^4	3.92×10^4		−70.3	−147
	K_2^{2-}	8.34×10^2	6.47×10^2	5.02×10^2		−36.2	−69.9
AQ	K	1.72	1.45	1.31		−19.3	−62.8
AQ^-	K^-	3.6×10^a	3.1×10^a	$2.1 \times 10^{a,c}$		-37^a	-100^a
AQ^{2-}	K_1^{2-}	1.15×10^5	7.33×10^4	$5.17 \times 10^{4\ c}$		−56.9	−101
	K_2^{2-}	4.52×10^2	3.10×10^2	2.78×10^2		−34.8	−70.3
CL	K		6.50×10^{-1}	5.80×10^{-1}	5.20×10^{-1}	−16.5	−59.8
CL^-	K^-	*b*	*b*	*b*	*b*	*b*	*b*
CL^{2-}	K_1^{2-}		3.30×10^3	3.79×10^3	1.61×10^3	−52.8	−112
	K_2^{2-}		2.09×10	1.79×10	1.32×10	−33.8	−89.7
BR	K			5.80×10^{-1}			
BR^-	K^-	*b*	*b*	*b*	*b*	*b*	*b*
BR^{2-}	K_1^{2-}			3.79×10^3			
	K_2^{2-}			1.79×10			

[a] Small values of $\Delta E_{1/2,1}$ and overlapping of the first and second waves in high [MeOH] region cause somewhat low precision in estimation of K^-. See the text for details. [b] Values are not estimated by the present method because of quite small values of $\Delta E_{1/2,1}$. See the text for details. [c] Values listed are somewhat different from the previous data.[12] These were corrected by the experiments performed several times.

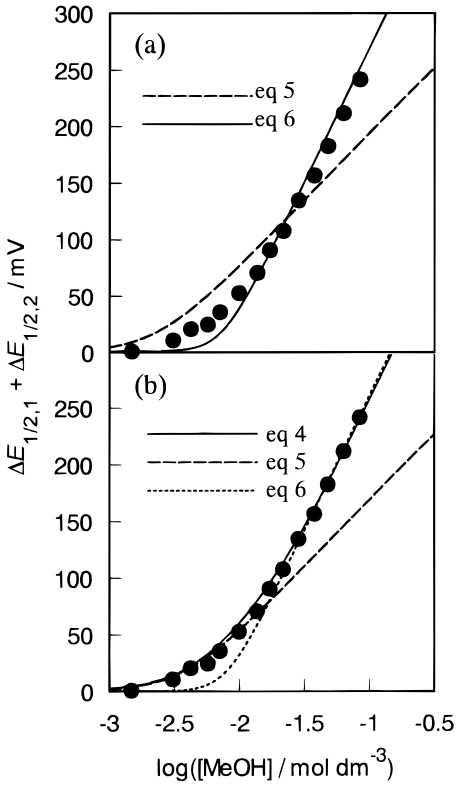

Figure 3. Dependence of the ($\Delta E_{1/2,1} + \Delta E_{1/2,2}$) values of BQ on concentrations of MeOH with the regression curves based on eqs 5 and 6 (a) and eq 4 (b). In (b) regression curves represented by a dashed line and a dotted line are obtained from the analyses based on eq 5 for the data obtained at lower [MeOH] than 1.48×10^{-2} M and based on eq 6 for the data obtained at higher [MeOH] than 1.85×10^{-2} M, respectively.

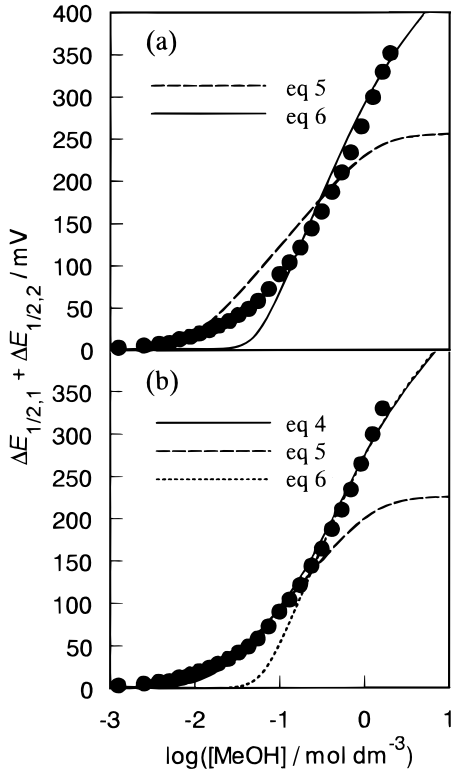

Figure 4. Dependence of the ($\Delta E_{1/2,1} + \Delta E_{1/2,2}$) values of CL on concentrations of MeOH with the regression curves based on eqs 5 and 6 (a) and eq 4 (b). In (b), regression curves represented by a dashed line and a dotted line are obtained from the analyses based on eq 5 for the data obtained at lower [MeOH] than 2.33×10^{-1} M and based on eq 6 for the data obtained at higher [MeOH] than 3.07×10^{-1} M, respectively.

electrochemistry provided the electronic spectra of BQ^{2-} and CL^{2-} in the absence and the presence of various concentrations of MeOH. Addition of a small amount of MeOH apparently caused a blue shift of the PQ^{2-} bands.

A typical example of the spectral behavior is illustrated in Figure 5a. The BQ^{2-} spectra do not give the isosbestic points on addition of high concentrations of MeOH, arising from coexistence of the 1:2 and 1:4 hydrogen-bonded complexes. The spectrum denoted by a solid line

Table 2. Observed Spectral Data and CNDO/S-CI Calculation Results for the Longest Wavelength Bands of BQ, BQ^{2-}, CL, and CL^{2-} and Their Hydrogen-Bonded Complexes with MeOH

	observed[a]	calculated			
compd	*E*/eV (λ/nm)	*E*/eV (λ/nm)	*f*[b]	CI[c] (%)	assignment[d]
BQ	5.12 (242)	5.31 (234)	0.885	92 ($b_{1u} \rightarrow b_{3g}$)	$^1B_{2u} \leftarrow {}^1A_g$
$BQ-(MeOH)_2$	5.10 (243)	5.37 (231)	0.959	93 ($b_{1u} \rightarrow b_{3g}$)	$^1B_{2u} \leftarrow {}^1A_g$
BQ^{2-}	3.46 (358)	3.43 (361)	0.211	93 ($b_{3g} \rightarrow a_u$)	$^1B_{3u} \leftarrow {}^1A_g$
$BQ^{2-}-(MeOH)_2$	*e*	3.80 (326)	0.174	91 ($b_{3g} \rightarrow a_u$)	$^1B_{3u} \leftarrow {}^1A_g$
$BQ^{2-}-(MeOH)_4$	3.85 (322)	3.95 (314)	0.159	89 ($b_{3g} \rightarrow a_u$)	$^1B_{3u} \leftarrow {}^1A_g$
CL	4.31 (288)	5.05 (246)	0.809	93 ($b_{1u} \rightarrow b_{3g}$)	$^1B_{2u} \leftarrow {}^1A_g$
$CL-(MeOH)_2$	4.31 (288)	5.06 (245)	0.823	93 ($b_{1u} \rightarrow b_{3g}$)	$^1B_{2u} \leftarrow {}^1A_g$
CL^{2-}	3.47 (357)	3.06 (405)	0.235	94 ($b_{3g} \rightarrow a_u$)	$^1B_{3u} \leftarrow {}^1A_g$
$CL^{2-}-(MeOH)_2$	*e*	3.30 (376)	0.226	94 ($b_{3g} \rightarrow a_u$)	$^1B_{3u} \leftarrow {}^1A_g$
$CL^{2-}-(MeOH)_4$	3.66 (339)	3.40 (365)	0.208	93 ($b_{3g} \rightarrow a_u$)	$^1B_{3u} \leftarrow {}^1A_g$

[a] Values at the maximum intensity in MeCN. [b] Oscillator strengths. [c] For example, ($b_{1u} \rightarrow b_{3g}$) means a singly excited configuration from the b_{1u} filled π-MO to the b_{3g} unoccupied π-MO. [d] Under D_{2h} symmetry. [e] Spectra of the $PQ^{2-}-(MeOH)_2$ complexes themselves are not observed. See the text for details.

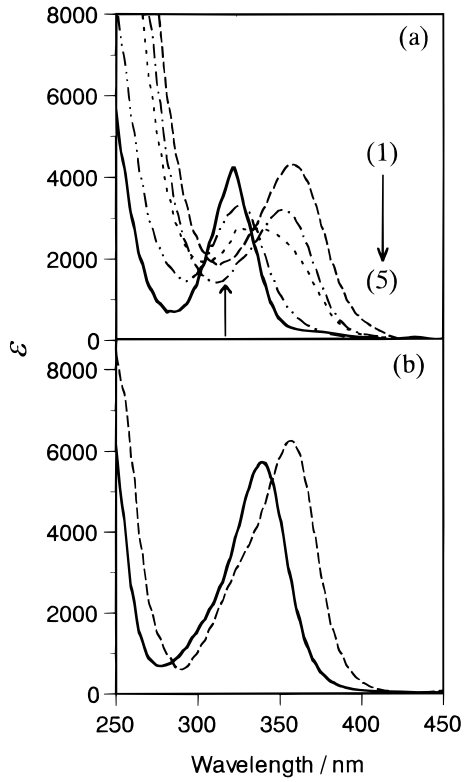

Figure 5. Electronic spectra of free and hydrogen-bonded BQ^{2-} and their mixtures (a) and of free and hydrogen-bonded CL^{2-} (b). (a) Arrows show direction of the spectral changes with increasing [MeOH]. The spectra of 1, 2−4, and 5 correspond to BQ^{2-} itself, a mixture of free and hydrogen-bonded BQ^{2-} and the $BQ^{2-}-(MeOH)_4$ complex itself, respectively. The spectrum 3 corresponds to the 30:69:1 mixture of free BQ^{2-}, the $BQ^{2-}-(MeOH)_2$ complex, and the $BQ^{2-}-(MeOH)_4$ complex. [MeOH] (M): (1) 0, (3) 6.80×10^{-3}, (5) 1.23. (b) The spectra represented by a dashed line and a solid line correspond to CL^{2-} and the $CL^{2-}-(MeOH)_4$ complex, respectively. [MeOH] (M): 0 (dashed line), 3.08 M (solid line).

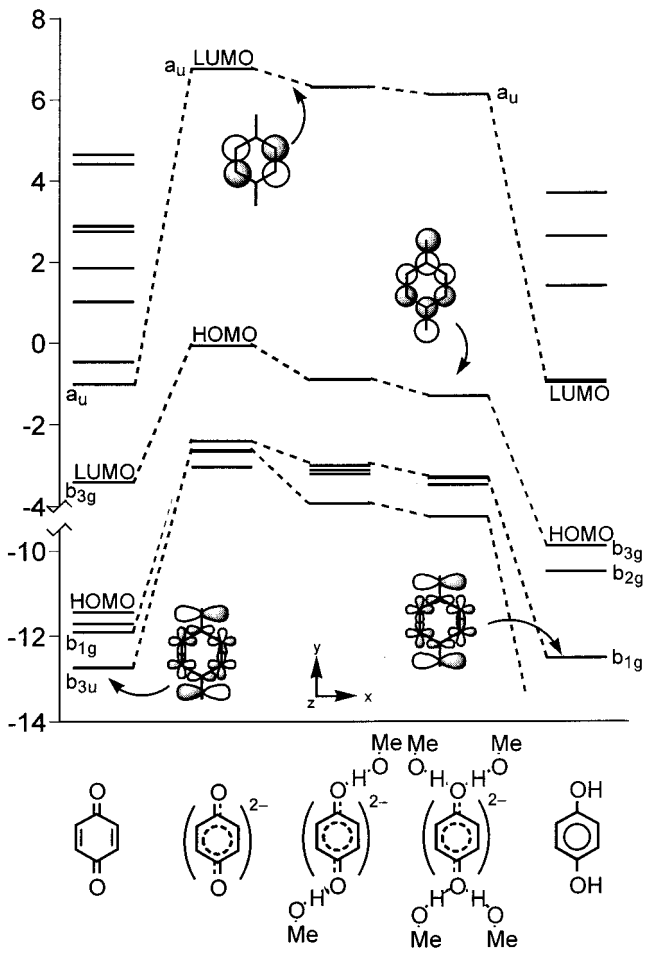

Figure 6. Energy levels and illustrations of the CNDO/S SCFMO related to the longest wavelength band of BQ, BQ^{2-}, the $BQ^{2-}-(MeOH)_2$ and $BQ^{2-}-(MeOH)_4$ complexes, and BQH_2.

in Figure 5a is ascribed to the 1:4 hydrogen-bonded complex itself. Indeed, the absorption maximum of the $BQ^{2-}-(MeOH)_4$ complex is in consonance with the published data for BQ^{2-} generated by deprotonation in EtOH.[33] A qualitatively similar but small effect of hydrogen bonding on the band is observed for CL^{2-}, as shown in Figure 5b. The blue shift of the CL^{2-} spectra is 0.19 eV, whereas that of BQ^{2-} is 0.39 eV. Certainly, the degree of the blue shift indicates the strength of hydrogen bonding to PQ^{2-}.

To treat the situation more quantitatively, CNDO/S-CI calculations were done. Table 2 lists the calculated and observed spectral data. The longest wavelength bands of BQ^{2-} and CL^{2-} are assigned to the $^1B_{3u} \leftarrow {}^1A_g$ transition contributed mainly from the HOMO−LUMO electronic configuration under D_{2h} symmetry, corresponding to the benzenoid ^1L_b state.[34] This indicates that the PQ^{2-} prefer a benzenoid structure rather than a quinoid form, which agrees well with the optimized geometries

(33) Kimura, K.; Yoshinaga, K.; Tsubomura, H. *J. Phys. Chem.* **1967**, *71*, 1, 4485.

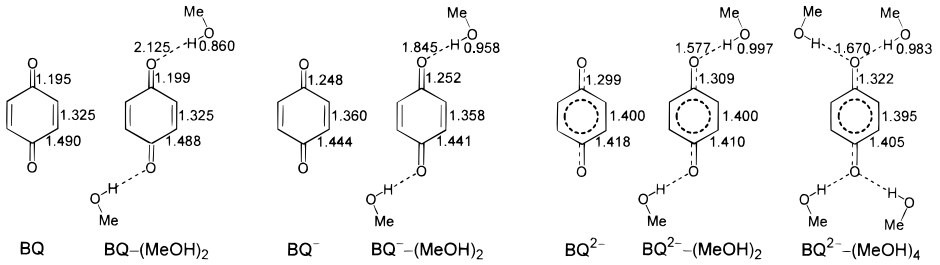

Figure 7. Optimized geometries of BQ, BQ^-, BQ^{2-}, and their hydrogen-bonded complexes with MeOH calculated by the RHF/6-31+G(d,p) or UHF/6-31+G(d,p) energy gradient method.

described in the next section and the resonance Raman spectroscopic results.[11] The BQ^{2-} and CL^{2-} bands are regarded as the benzenoid bands red-shifted by the substituent effect of strongly electron-donating substituents. The calculation results reproduce the difference in the degree of the experimental blue-shift between BQ^{2-} and CL^{2-}. Figure 6 shows the calculated MOs concerning the electronic transitions of BQ and BQ^{2-}. The active MO of BQ^{2-} to the hydrogen bonding is the b_{3u} and b_{1g} lone pair orbitals localized on the carbonyl oxygen atoms, which is sufficiently activated to accept hydrogen with two-electron reduction. The activation of the b_{3g}-HOMO of BQ^{2-} as well as the lone pair orbitals is weakened by the hydrogen bonding of BQ^{2-} with MeOH, as illustrated in Figure 6. The blue-shift in the BQ^{2-} spectra is attributable to the remarkable stabilization of the b_{3g}-HOMO with the hydrogen-bond formation. This is considered to be the same behavior as the blue shift in intramolecular charge-transfer bands observed for heterocyclic amine *N*-oxides because the excited state of BQ^{2-} mainly arises from the $b_{3g} \rightarrow a_u$ configuration of a typical intramolecular charge-transfer state.[35] It is reasonably understood that the HOMO → LUMO transition of BQH_2 as the most strongly interacted model appears at a wavelength shorter than that of the hydrogen-bonded complex, as shown in Figure 6. The considerable effect of the hydrogen bonding on the π-electron distribution in BQ^{2-} is suggested despite the negligible π-type charge-transfer (CT) by hydrogen bonding.

Geometries of PQ^{2-} and the Hydrogen-Bonded Complexes with MeOH. The geometry changes on going from PQ to PQ^{2-} and the hydrogen-bonded complexes were calculated. A typical example of the results is illustrated in Figure 7. The C═O bond distances are of a typical double bond for neutral PQ and of a single bond for PQ^{2-}, while those for PQ^- are between. The C═C bonds are elongated, but the C−C bonds are contracted with sequential reduction of PQ, indicating that the quinoid form changes to a benzenoid ring. The structure of PQ^{2-} is, therefore, characterized by a lengthening of the C═O bond (formal single bond) and a dissolution of the bond alternation in the quinoid structure. This propensity is slightly exhibited in the structure of PQ^-, as shown in the published results for BQ^- at various levels of MO calculations.[11,12,14] No major changes are brought about in the internal geometries of PQ, PQ^-, and PQ^{2-} molecules as a result of hydrogen bond formation. The only significant change is a slight lengthening of the C═O bond, particularly in the case of PQ^{2-} in which the distance is slightly shorter than 1.381 Å of hydroquinone.[36] The hydrogen-bond distances, however, significantly change with the redox states of PQ. The O···O distances of the 1:2 hydrogen-bonded complexes of PQ^{2-} are considerably shorter than 2.8 Å which is estimated from the various hydrogen-bonded complexes containing the O···H−O moiety.[27] It is indicated that hydrogen bonds strengthen upon reduction of PQ to PQ^- to PQ^{2-}. The distances of the 1:4 complexes are slightly longer than those of the 1:2 complexes. This is due to steric crowding of the 1:4 complexes.

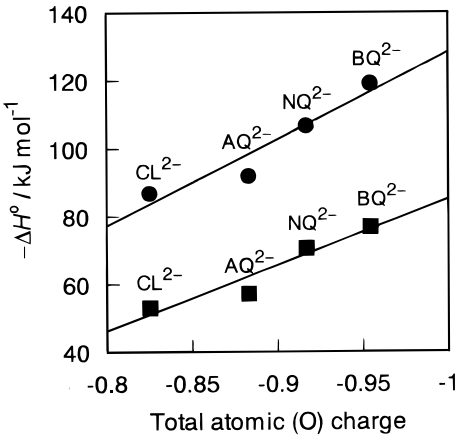

Figure 8. Dependence of the observed $\Delta H°$ values upon atomic gross charge on the carbonyl O atoms of PQ^{2-} calculated by the RHF/6-31G(d) method. The $\Delta H°$ values correspond to the reactions of $PQ^{2-} + 2MeOH \rightarrow PQ^{2-}-(MeOH)_2$ (●) and $PQ^{2-} + 4MeOH \rightarrow PQ^{2-}-(MeOH)_4$ (■).

n−σ CT Interaction in the Hydrogen Bonds of PQ^{2-} with MeOH. It is well recognized that hydrogen bonds are substantially electrostatic in nature, whereas n−σ charge-transfer interaction plays an important role in their directionality and strength.[29,37] Indeed, the formation energies of BQ^{2-} with MeOH are qualitatively explained by atomic charge on the carbonyl oxygen atoms, as shown in Figure 8. Table 3 lists the hydrogen-bond energies and the magnitude of the CT calculated for the PQ^{n-} (n = 0, 1, 2) and MeOH systems. Upon reduction of PQ to PQ^- to PQ^{2-}, the CT through the hydrogen bonds is magnified and the formation energies become large. These are in good agreement with the experimental results and the optimized geometries. Figure 9 shows the total atomic charge for BQ^{2-} and the hydrogen-bonded complexes. The atomic charge is closely concerned in the π-electron distribution. Although the

(34) Jaffé,H. H.; Orchin, M. *Theory and Applications of Ultraviolet Spectroscopy*; John Wiley and Sons: New York, London, 1962; Chapter 9.

(35) Yamanaka, M.; Kubota, T.; Akazawa, H. *Theor. Chim. Acta* **1969**, *15*, 224.

(36) Sakurai, T. *Acta Crystallogr.* **1968**, *B24*, 403.

(37) Morokuma, K. *Acc. Chem. Res.* **1977**, *10*, 294.

Table 3. Formation Energies and Charge Migration of the Hydrogen-Bonded Complexes of PQ, PQ^- and PQ^{2-} with MeOH Calculated by the RHF/6-31G(d) or UHF/6-31G(d) Methods

	ΔE/kJ mol^{-1} [a,b]		
complexes	SCF	MP2	ΔQ[c]
$BQ-(MeOH)_2$	−41.2 (−42.6)	−58.7 (−59.0)	0.040
$BQ^--(MeOH)_2$	−107 (−93.1)	−139 (−117)	0.105
$BQ^{2-}-(MeOH)_2$	−226 (−188)	−269 (−217)	0.231
$BQ^{2-}-(MeOH)_4$	−400 (−335)	−482 (−398)	0.358
$NQ-(MeOH)_2$	−40.2	−56.0	0.032
$NQ^--(MeOH)_2$	−96.7	−124	0.081
$NQ^{2-}-(MeOH)_2$	−194	−229	0.175
$AQ-(MeOH)_2$	−41.9	−59.3	0.026
$AQ^--(MeOH)_2$	−90.6	−117	0.069
$AQ^{2-}-(MeOH)_2$	−173	−198	0.143
$CL-(MeOH)_2$	−24.6	−39.0	0.018
$CL^--(MeOH)_2$	−72.1	−93.8	0.052
$CL^{2-}-(MeOH)_2$	*d*	*d*	*d*
$CL^{2-}-(MeOH)_4$	−233	−305	0.181

[a] The hydrogen-bonded complex formation energy (ΔE) is calculated by the equation: $\Delta E = E(PQ-(MeOH)_n) - E(PQ) - n(E(MeOH))$, where E denotes the total energy of the molecule shown in parentheses.[29] [b] Values in parentheses are calculated with 6-31+G(d,p) basis sets. [c] The magnitude of CT is expressed by charge migration ΔQ: $\Delta Q = Q$(PQ, complexed) − Q(PQ, free), where Q is the sum of gross population of all atoms in the molecule shown in parentheses.[29] [d] Energy gradient calculations failed to get the optimized geometry.

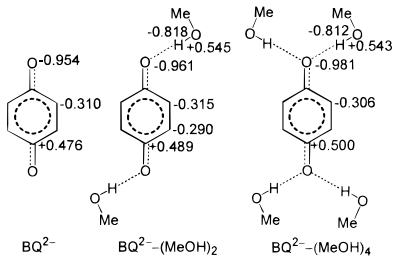

Figure 9. Atomic gross charge of BQ^{2-} and the 1:2 and 1:4 hydrogen-bonded complexes with MeOH calculated by the RHF/6-31G(d) method.

charge transfer occurs from the b_{1g} and b_{3u} lone pair orbitals of the carbonyl oxygen atoms to the MeOH (i.e., n−σ CT interaction), the CT interaction significantly affects the MO energies and the electron distribution of the π-electronic system of BQ^{2-}, as shown in Figures 6 and 9. The electron-transfer ability of BQ^{2-} is therefore controlled by hydrogen bonding involving n−σ CT interaction because the π-HOMO of BQ^{2-} plays an important role in the redox-mediated electron transfer of BQ. Although π-type CT is negligible, a considerable effect of hydrogen bonding on the functions and properties of BQ^{2-} has been suggested. The comparison of the spectral change between BQ (Figure 2) and BQ^{2-} (Figure 5a) experimentally exhibits the difference in effect of hydrogen bonding on the π-electronic system of the quinone.

Conclusions

Electrochemistry and spectroelectrochemistry of PQ combined with ab initio MO calculations have provided a clear description of the molecular and electronic structures of the hydrogen-bonded complexes of PQ^{2-} with MeOH. The n−σ type CT interaction has an important role in the hydrogen bonds of PQ^{2-}. The blue-shift of the PQ^{2-} spectra evidently displays the strength of hydrogen bonding involving n-σ CT interaction. These results serve as basic information on the effect of hydrogen bonding on the biological function of quinone dianions. It is suggested that the differing functions and properties of biological quinone dianions are conferred by hydrogen bonding involving the CT interaction with their protein environment. In addition, further inspection of this model can give deeper insight into the characterization of the electrogenerated active dianions and electron-transfer coupled with proton transfer in quinone−hydroquinone redox systems.

Acknowledgment. We thank the Computer Center of Institute for Molecular Science, Okazaki National Research Institute, for the use of the NEC HSP computer and library program Gaussian98. This work was supported by a Grant-in-Aid for Scientific Research on Priority Areas Nos. 05235240, 06226270, and 07215273 and a Grant-in-Aid for Scientific Research No. 11672148 from the Ministry of Education, Science, Sports and Culture of Japan.

Supporting Information Available: A table of optimized geometries for PQ, PQ^-, and PQ^{2-} and their hydrogen-bonded complexes. This material is available free of charge via the Internet at http://pubs.acs.org.

JO991590Q